Disorder effects in angle-resolved photoelectron spectroscopy*

N. J. Shevchik
Department of Physics, State University of New York, Stony Brook, New York 11794
(Received 6 April 1977)

The effects of compositional, vibrational, long-range positional, and topographical disorders upon the angle-resolved photoemission spectra of tightly bound valence electrons are investigated. In order to take into account the strong potential sensed by the electron in the vicinity of the atomic core, an augmented-plane-wave final state is employed. With this final state, the interference between atoms in the optical ionization step is identical to that obtained with a plane-wave final state, but the atomic cross sections are those calculated from spherical, not plane waves. The angle-energy dependence of the photoemission spectra of crystalline alloys depends upon the degree of chemical ordering, the concentration, and the atomic photoionization cross sections of each element present. The primary effect of spatial disorder is to weaken k conservation in the optical ionization step, particularly as the momentum of the final state increases. It is found that phonon disorder is not important in the ultraviolet-photoemission (UPS) regime, but it is sufficient to destroy almost totally k conservation in the x-ray-photoemission (XPS) regime in most materials at room temperature. In this limit, the observed angle-resolved spectra ought to reveal the total density of states modulated by atomic-like photoionization cross sections. High-order phonon induced optical transitions might limit the energy resolution obtainable in the XPS regime to a few tenths of an electron volt. Surface roughness is shown to weaken the conservation of the component of the momentum parallel to the surface, possibly even in the XPS regime. Topographical disorder is important as long as refraction of the photoelectron at the surface remains large. It is argued that if the final electron states are very heavily mixed plane waves, then surface roughness and refraction are much more important than when the states are free-electron-like. Photoemission spectra of electrons directed along a crystallographic axis are shown to provide an important test for determining the validity of several recent models for the final electron state.

I. INTRODUCTION

Many recent angle-resolved photoemission spectra[1-7] have been interpreted largely in terms of models based upon the assumptions of (i) a plane-wave final electron state, and (ii) k conservation in the optical excitation and transport steps. It is not clear, however, that either of these assumptions is valid in describing the experimental spectra in general.

The assumption of a plane-wave final state at first seems reasonable, since as the photoelectron moves more quickly at high energies, it ought to feel the crystal potential less strongly. Wagner *et al.*[2] have shown that cross sections calculated from plane-wave final states fail to reproduce the photoemission spectra directed along crystallographic axes of the noble metals. Recently, it has been suggested that since the wave function in the vicinity of the atomic core makes the main contribution to the photoionization cross sections at high energies, a plane-wave final state is inadequate for describing the angular dependence of the cross sections.[7,8]

We expect k to be conserved in the optical ionization step only when the atoms are arranged in a perfectly periodic array, and we expect the component of the electron momentum parallel to the surface to be conserved only when the surface of the crystal is perfectly smooth.[9-11] In real crystals, however, neither of these conditions is achieved. Defects, such as dislocations and vacancies, might occur within the bulk. The surface of a real crystal is likely to be irregular and rough on an atomic scale, particularly after it has been subjected to mechanical polishing or argon-ion bombardment. Even in crystals that lack such defects, the atoms do not sit at well-defined points, but they vibrate weakly about their equilibrium positions. In amorphous solids, liquids, and some compositionally disordered alloys, k is not a rigorous quantum number for the initial electron states[12] and k conservation should not be a strong constraint in the photoemission process.

In this paper, we are concerned with the effects of bulk and surface disorder upon the angle-resolved photoelectron spectra of solids and the extent to which they modify the applicability of the theories developed for ideal situations.[9-11] The structure of the paper is as follows:

In Sec. II, we argue that the free-electron plane wave provides a totally inadequate description for the final electron state, and that an augmented-plane-wave (APW) final state does a better job. The consequences of the APW final state are that the optical transitions are atomic-like in nature, while the escape and transport steps are mostly free-wave-like in nature.

In Sec. III, we consider the influence of thermal vibrations upon the optical ionization steps by em-

ploying a theory similar to that used in x-ray diffraction. We find that at room-temperature phonon disorder, in general, is not very important in the ultraviolet-photoemission-spectrum (UPS) regime, where the momentum of the final state is small; however, in the x-ray-photoemission spectrum (XPS) regime, where the momentum of the final state is large, it nearly totally destroys k conservation. In this limit, the angle-resolved photoemission spectra reveal the total density of states modulated by atomic-like photoionization cross sections. We also find that the phonon disorder might lead to an energy broadening of valence-band spectra by as much as a few tenths eV in the XPS regime.

In Sec. IV, we consider the effects of compositional disorder, such as that occurring in crystalline alloys. We point out that the angular photon-energy dependence of the spectra is sensitive to the chemical order, thus, photoemission can be used to determine chemical clustering effects in a manner similar to that employed in x-ray diffraction.

In Sec. V, we show that long-range positional disorder, such as that occurring in liquids and amorphous solids, destroys k conservation in the optical-transition step, even for photon energies in the UPS regime.

In Sec. VI, we consider the effects of disorder on the passage of the electron through the surface barrier. Perturbations of the surface plane induced by phonon disorder are not important for any final-state energy. However, surface roughness and random coverage by adsorbates can destroy the conservation of momentum at the surface for photon energies in the UPS regime and also in the XPS regime, provided that the final state at high energy is Bloch-like.

In Sec. VII, we discuss the importance of topographical disorder, in which the surface is broken up into several smaller planes that are aligned in different directions. It appears that refraction of the photoelectron at such planes might seriously smear the angle-resolved spectra for photon energies extending into the XPS regime.

Finally, in Sec. VIII we discuss the case of photoemission directed along a crystallographic axis and how it can serve to test the validity of some of the final-state models proposed recently.

II. INITIAL AND FINAL STATES

In this section, we consider the nature of the initial and final electronic states. We assume that the charge density of the initial electron state follows the motion of the atomic cores, whether the disorder is of a dynamic (phonons) or a static nature. For crystalline solids containing one atom per unit cell, the wave function having reduced momentum k_i can be written in the tight-binding approximation as[13,14]

$$\psi_{\vec{k}_i}(r)=\sum_m \exp(i\vec{k}_i\cdot\vec{R}_m)\phi_{\vec{k}_i}(\vec{r}-\vec{R}_m)\,, \tag{1}$$

where R_m is the position of the coordinate of atom m and $\phi(r)$ is a linear combination of atomic orbitals. We point out that it would be cumbersome to describe the initial state in terms of a plane-wave expansion for an arbitrary set of R_m's. If slight deviations away from the crystalline equilibrium positions are considered, the Fourier transform of (1) would contain a very large number of terms, rather than a few as in the case of perfect order.

The description of the final state presents a more difficult problem than the initial state. It has been pointed out earlier that the plane-wave final-state wave function fails to describe the photoemission spectra directed along various crystallographic axes[2,7] since it cannot reproduce the correct spherical symmetry of the wave function in the region of the core, the region that contributes the most to the photoionization cross sections, particularly as the photon energy increases.[8,15-17]

When the interaction between the electromagnetic field and the electron is written as

$$H'=(e/mc)\vec{A}\cdot\vec{P}e^{i\omega t}\,,$$

where $\vec{A}$ is the electromagnetic potential and $\vec{P}$ is the momentum of the electron, the matrix element connecting some initial state, $\phi'(r)$, with the plane-wave final state of momentum k_f is[11]

$$M_{fi}=(e/mc)\vec{A}\cdot\vec{k}_f\tilde{\phi}(\vec{k}_f)\,, \tag{2}$$

where $\tilde{\phi}(\vec{k}_f)=\int e^{i\vec{k}_f\cdot\vec{r}}\phi'(r)\,d^3r$. A convenient feature of the plane-wave final state is that the matrix element is proportional to the Fourier transform of the initial state.[11] When the charge density of the initial state vanishes in the direction of k_f, so does the matrix element.

An obvious and serious defect of the plane-wave final state is exposed when we consider the emission from an isolated atomic orbital. Eq. (2) predicts that only the atomic orbital having $m=0$ with respect to the direction of emission can contribute to the spectra. This constraint is much more restrictive than the optical-transition rules valid for spherical symmetry, i.e., $\Delta l=\pm1$, $\Delta m=0,\pm1$. The plane-wave final state can be rigorously valid only in the limit that the atomic potentials vanish. Unfortunately, in this limit the initial states also be-

come plane waves, which have a vanishing photoionization cross section. The initial states can have a nonvanishing cross section only when the atomic potential exists. Since the atomic potential is responsible for the cross sections, one should also expect the optical-selection rules to be governed by the spherical symmetry of that potential. Therefore, it is clear that the plane-wave final state is never valid for describing angular dependence of the photoionization cross sections, even at extremely high photon energies and arbitrarily weak atomic potentials. The polarization dependence given by Eq. (2) is also incorrect for similar reasons. (The length matrix element calculated with a plane-wave final state gives selection consistent with spherical symmetry.)

It is crucial to determine whether the final electron state in the solid has planar or spherical symmetry. Since the wave functions in the region of the atomic core makes the primary contribution to the photoionization cross section at large energies, a final state that describes this portion of the wave function well is needed, even when the atoms are in crystals.

Since the photoionization matrix element can be regarded approximately as the sum of the atomic matrix elements, it is not at all obvious how the interaction between atoms can make valid the plane-wave final state, when it is not valid for the isolated atom.

However, the description of the photoionization cross section is only half the problem: We must also consider the escape process of the photoelectron, and therefore, the wave function in the vicinity external to the core.[9,10] In this region, where the potential varies more smoothly, a plane-wave final state might be appropriate. We therefore suggest that a single augmented-plane-wave (APW) function, which takes into account the strong potential of the atomic cores,[14] provides a more suitable description of the final electron state than the single-plane-wave state. We recognize that the crystal potential can mix the APW's together, particularly at low energies. However, we ignore this complication, since a single APW ought to illustrate at least the qualitative effects of the disorder.

The APW final state can be written as[14]

$$\psi = e^{i\vec{k}_f\cdot\vec{r}} + \sum_m \exp(i\vec{k}_f\cdot\vec{R}_m)\Phi(\vec{r}-\vec{R}_m), \tag{3}$$

where k_f is the wave vector of the final state, the magnitude of which is given by the free-electron energy dispersion. The function in the sum describes the state in the vicinity of the atomic core and is given by,

$$\Phi(r) = \begin{cases} \sum_{l=0}^{\infty} i^l(2l+1)\left(\frac{j_l(k_f a)}{R_l(a,E_f)}R_l(r,E_f) - j_l(k_f r)\right) \\ \quad \times P_l(\cos\theta) \text{ for } r<\tilde{a} \\ \quad 0 \text{ for } r>\tilde{a}\,, \end{cases} \tag{4}$$

where $j_l(kr)$ is a spherical Bessel function, $\tilde{a}$ is the muffin-tin radius, and θ is the angle between the position coordinate r and k_f. The function $R_l(r,E)$ is the solution to the radial equation[14]

$$\left[-\frac{1}{r^2}\frac{\partial}{\partial r}\left(r^2\frac{\partial}{\partial r}\right)+\frac{l(l+1)}{r^2}+V(r)\right]R_l(r,E_f) = E_f R(r,E_f), \tag{5}$$

where $V(r)$ is the self-consistent potential of the atom. We note that $\phi(r)$ is the amount by which the wave function deviates from a single plane wave and that it contains only spherical harmonics for which $m=0$.[13,14] As we shall discuss in Sec. VIII, this might be a serious defect for all models based upon planar symmetry.

When the APW is written as in (3), it appears to be a plane wave plus a linear combination of atomic (or spherical) orbitals. The fraction of of time that it is atomic-orbital-like is

$$\lambda = \tilde{a}^3/r_1^3\,, \tag{6}$$

where r_1 is the interatomic spacing. The radius $\tilde{a}$ should be given roughly as the distance at which the kinetic energy of plane-wave state E_f is equal to the self-consistent atomic potential, $V(r)$. As E_f increases, we expect $\tilde{a}$ to decrease and the total wave function to look more like a plane wave, and less like a spherical wave.

The Fourier transform of the APW function has the approximate form

$$\tilde{\psi}(\vec{k}) = \delta(\vec{k}-\vec{k}_f)(1-\lambda) + \sum_m \exp[i(\vec{k}-\vec{k}_f)\cdot\vec{R}_m] \times \sum_{l=0}^{\infty}\frac{i^l(2l+1)}{R_l(a)}j_l(k_f a)P_l(\cos\theta)\tilde{R}_l(k)\,. \tag{7}$$

The first portion, due to the plane-wave part, constitutes the primary component of the final state at higher photon energies; it should dominate the escape and transport steps of the photoemission process. The second part, due to the core regions, has Fourier components in several directions, which in addition to contributing to the photoionization cross section, also contribute "secondary cones" to the escape processes.[9]

The probability that the initial tight-binding state of momentum k_i makes a transition into an APW final state of momentum k_f is

$$|M_{fi}|^2 = |\sigma_i(\vec{k}_f)|^2 S(\vec{k}_f-\vec{k}_i)\delta(E_f-E_i-\hbar\omega)\,, \tag{8}$$

where

$$S(\vec{k}) = \sum_{m,n} \exp[i\vec{k}\cdot(\vec{R}_m - \vec{R}_n)] .$$

The indices m and n extend over all of the atomic sites that can contribute to the elastic photoemission current and $\sigma_i(\vec{k}_f)$ is the photoionization cross-section matrix element for the atom calculated from the APW's. The δ function insures that energy is conserved in the photoionization step. The result is the same as that derived from a single-plane-wave final state, except that the atomic photoionization cross sections are those derived from spherical, not plane waves. The summation over the lattice positions $S(k)$ is the familiar interference function (or structure factor) that occurs in diffraction theory.[18-19] In this context we might visualize photoemission as a diffraction process, in which the initial state of momentum k_i is the incident beam and the final state of momentum k_f is the scattered beam. However, in contrast to the usual diffraction theories, the magnitudes of the momenta of the initial and final states are different.

When perfect order exists, the summation in Eq. (8) yields the usual conservation of momentum constraint,[9-11] i.e.,

$$\vec{k}_f - \vec{k}_i + \vec{G} = 0 ,$$

where G is a reciprocal-lattice vector. An equivalent statement of this constraint is that the reduced momentum of the final state is equal to that of the initial state.

The result in Eq. (8) is valid only for a static structure. When the positions of the atoms depend upon time, the matrix element connecting the initial and final state can be written as

$$M_{fi} = \int_{-\infty}^{\infty} \sum_{m} \exp[i\Delta\vec{k}\cdot\vec{R}_m(t)]\sigma_m(\vec{k}_f) \times \exp[i(E_f - E_i - \hbar\omega)t/\hbar]dt . \quad (9)$$

The integration over time insures that energy is conserved in the optical-transition step. The expectation value for the transition probability becomes

$$|M_{fi}|^2 = |\sigma_i(\vec{k}_f)|^2 S(\Delta\vec{k}, (E_f - E_i - \hbar\omega)/\hbar) , \quad (10a)$$

where

$$S(\Delta\vec{k}, \omega_s) = \int_{-\infty}^{\infty} \sum_{m,n} \exp i\Delta\vec{k}\cdot[\vec{R}_m(0) - \vec{R}_n(t)] \times \exp(i\omega_s t)\, dt . \quad (10b)$$

In deducing Eqs. (10a) and (10b), we have used the fact that the correlations in the positions do not depend upon the absolute value in time. This is why the time of R_m is taken to be $t = 0$. The quantity $\hbar\omega_s$ is the amount of energy supplied by the lattice to the optical-ionization step. We have assumed in deriving Eq. (10) that the energies of the initial and final states do not depend strongly upon the positions of the atoms. This assumption is probably valid only for weak phonon disorder.

In the remainder of this paper, we shall be concerned with the effects of disorder upon the interference term in the photoionization cross section in Eqs. (8) and (10). We presently neglect the finite mean-free path of the photoelectron and other details of the escape process, since these are complications that would otherwise obscure the intended transparency of the formalism to be presented.

III. VIBRATIONAL DISORDER

In this section, we consider the effects of thermal vibrations in crystalline solids upon the k-conservation constraint. Following previous workers,[18,19] the position of atom m at time t can be written as

$$\vec{R}_m(t) = \vec{R}'_m + \vec{U}_m(t) , \quad (11)$$

where R'_m is the equilibrium position and $U_m(t)$ is the displacement of the atom m. Since the atoms are moving, we must consider the dynamic structure factor as given in Eq. (10), which can be written as

$$S(\Delta\vec{k}, t) = \sum_{m,n} \exp[i\Delta\vec{k}\cdot(\vec{R}'_m - \vec{R}'_n)] \times \exp\{+ i\Delta\vec{k}\cdot[\vec{U}_m(0) - \vec{U}_n(t)]\} , \quad (12)$$

where $\Delta\vec{k} = \vec{k}_f - \vec{k}_i$. Performing an average which eliminates terms that are odd in the displacements, we obtain

$$S(\Delta\vec{k}, t) = \sum_{m,n} \exp[i\Delta\vec{k}\cdot(\vec{R}'_m - \vec{R}_n)] \times \exp(-\tfrac{1}{2}\{\Delta\vec{k}\cdot[\vec{U}_m(0) - \vec{U}_n(t)]\}^2) . \quad (13)$$

In order to evaluate the exponential factor in Eq. (13) we must consider the normal vibrational modes (phonons) of the solid. In terms of the phonon modes, the displacement of atom m can be written as

$$\vec{U}_m(t) = \sum_{j,q} \exp(i\vec{q}\cdot\vec{R}'_m - i\omega_{qj}t)a_{qj}\vec{\epsilon}_{qj} , \quad (14)$$

where a_{qj} and $\vec{\epsilon}_{qj}$ are the amplitude and displacement direction of the phonon mode having wave vector q and displacement index j.

Using Eq. (14), we obtain for the square of relative displacement of two atoms in the direction of the momentum transfer

$$\{\vec{\epsilon}_{\Delta k}\cdot[U_m(0) - U_n(t)]\}^2 = \sum_{qj} |a_{qj}|^2 (\vec{\epsilon}_{qj}\cdot\vec{\epsilon}_{\Delta k})^2 \times \{1 - \cos[\vec{q}\cdot(\vec{R}'_m - \vec{R}'_n)]\cos(\omega_{qj}t)\} , \quad (15)$$

where $\vec{\epsilon}_{\Delta k}$ is the unit vector in the direction of $\Delta\vec{k}$. The time-dependent structure correlation factor becomes

$$S(\Delta\vec{k}, t) = e^{-M} \sum_{n,m} \exp[i\Delta\vec{k} \cdot (\vec{R}'_n - \vec{R}'_m)] \exp\left(+ \Delta k^2 \sum_{qj} |a_{qj}|^2 (\vec{\epsilon}_{qj} \cdot \vec{\epsilon}_{\Delta k})^2 \cos(\vec{q} \cdot (\vec{R}'_m - \vec{R}'_n)) \cos(\omega_{qj} t) \right), \quad (16)$$

where

$$M = (\Delta k)^2 \sum_{qj} |a_{qj}|^2 (\vec{\epsilon}_{qj} \cdot \vec{\epsilon}_{\Delta k})^2 . \quad (17)$$

Expanding the summation in the exponential, retaining only the first two terms and performing the Fourier transform over time, we find that

$$S(\Delta\vec{k}, \omega_s) \cong e^{-M} \sum_{\vec{G}} \delta(\Delta\vec{k} - \vec{G}) \delta(\omega_s) + e^{-M} \sum_{qj} \Delta k^2 |a_{qj}|^2 (\vec{\epsilon}_{qj} \cdot \vec{\epsilon}_{\Delta k})^2 \times \sum_{\vec{G}} \delta(\Delta\vec{k} + \vec{q} - \vec{G}) \delta(\omega_s \pm \omega_{qj}) . \quad (18)$$

The first term corresponds to the usual k conservation in crystals, but it is reduced in strength by the Debye-Waller exponential term.[18,19] The second term, similar to the first-order thermal diffuse scattering obtained in x-ray diffraction theory, shows more explicitly how the phonons supply both energy and momentum to the electronic optical-excitation process. The phonon energy is only a few tens of millivolts, so that it does not seriously alter the energy of the electronic transition. In general, there is always a phonon of a proper wavelength to ensure that every initial state in the Brillouin zone can couple to the final state with the aid of a phonon. The amplitude of phonon mode q,j is given by[18,19]

$$\langle a_{qj}^2 \rangle = \frac{\hbar}{\omega_{qj} M_a} \left(\frac{1}{e^{-(\hbar/k_\beta T)\omega_{qj}} + \frac{1}{2}} \right) , \quad (19)$$

where M_a is the mass of the atom. At temperatures higher than the phonon frequency, the above becomes

$$\langle a_{qj}^2 \rangle \cong \frac{k_\beta T}{c^2 q^2 M_a} , \quad (20)$$

where c is the speed of sound. The probability for an optical transition involving the scattering of the electron from a phonon is given by

$$|\sigma_i(\vec{k}_f)|^2 \frac{\Delta k^2}{c^2 M_a} e^{-M} \frac{k_\beta T}{|\Delta k - \vec{G}_0|^2} |\vec{\epsilon}_{qj} \cdot \vec{\epsilon}_{\Delta k}|^2 \times \delta(E_f - E_i \pm \hbar\omega_{qj} - \hbar\omega) , \quad (21)$$

where $\vec{G}_0$ is the reciprocal lattice vector that is the closest to Δk. Since the phonons with the smallest wave vectors have the largest amplitudes, the first-order transitions involving the smallest deviations away from k conservation are the most probable. The first-order thermal diffuse contribution rises linearly with T, then decreases as the Debye-Waller factor decreases and higher-order terms in Eq. (16) become more probable. The contributions from higher-order phonon processes can be found by expanding Eq. (16) further.

The above analysis provides a picture of the effects of phonon disorder in reciprocal space. Now let us consider these effects in real space for a cubic system, but in order to do this it is convenient to ignore the time variations of the lattice and concentrate on the destruction of k conservation.

Assuming that all phonons have the same velocity and that the Brillouin zone is spherical, it can be shown that[18]

$$\langle [(\vec{U}_n - \vec{U}_m) \cdot \vec{\epsilon}_{\Delta k}]^2 \rangle = 2U_0^2 [1 - \gamma(k_0 R_{mn})] , \quad (22)$$

where

$$\gamma(x) = \frac{1}{x} \int_0^x \frac{\sin u}{u} \, du$$

and $k_0 = \pi/r_1$. As shown by James,[19] the square of the amplitude of the thermal vibrations of the atom about its equilibrium position is given by

$$U_0^2 \cong (3\hbar^2 / M_a k_\beta \Theta_m^2) T , \quad (23)$$

where Θ_m^2 is the average Debye x-ray temperature.

In terms of Eq. (22) the static structure factor can be written as

$$S(\Delta\vec{k}) = N + e^{-\Delta k^2 U_0^2} \times \sum_{n \neq m} \exp[i\Delta\vec{k} \cdot (\vec{R}'_m - \vec{R}'_n) + \gamma(k_0 R_{mn}) \Delta k^2 U_0^2] . \quad (24)$$

The function $\gamma(r)$, which is plotted in Fig. 1, expresses the effects of correlations on the relative motion of the atoms. Since $\gamma(r)$ approaches zero for large relative separations, the motion of atoms far apart is completely uncorrelated, while the relative displacements of nearest-neighbor atoms is about the average displacement of the atoms. Thus, the interference between atoms far apart is more sensitive to the thermal vibrations than that between nearest-neighbor atoms.

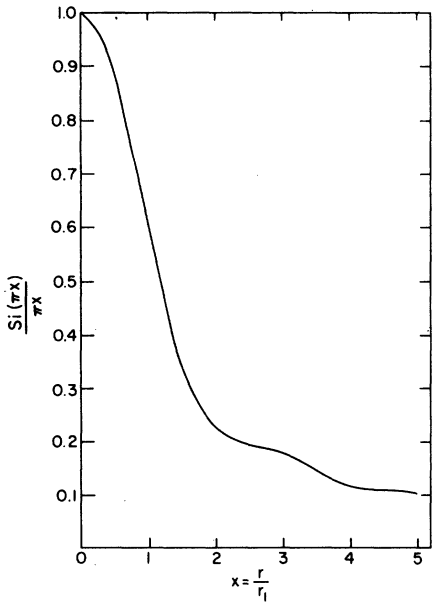

FIG. 1. Plot of the function $[\mathrm{Si}(\pi x)/\pi x]$. The quantity x is the ratio of the separation between atoms, r, to the nearest-neighbor separation, r_1.

In the limit that the correlations between the atoms can be neglected, i.e., $\gamma(r)\to 0$ for all r, Eq. (24) becomes the simple Debye model,[19]

$$S(\Delta\vec{k}) = N[1-\exp(-\Delta k^2 U_0^2)] + \exp(-\Delta k^2 U_0^2)\sum_G \delta(\Delta\vec{k}-\vec{G}) . \quad (25)$$

In Appendix A, we consider the time-dependent analog of Eq. (25). In contrast to the result in Eq. (18), the above is valid to all orders of Δk. The last term corresponds to the usual optical transitions in which k is conserved and the first term corresponds to transitions in which the electron momentum is not conserved. This expression tells us that the optical transitions from initial states in the Brillouin zone involving the largest transfer of momentum are the ones most likely to appear as non-k-conserving transitions. As the temperature and the final-state momentum increases, the strength of k-conserving transitions is reduced and when $U_0\Delta k\sim 1$, the non-k-conserving thermal diffuse transitions become dominant. In the limit that $U_0\Delta k \gg 1$, the atoms can be regarded as emitting electrons completely incoherently of one another.

The only restriction remaining upon the photoelectron intensity is due to the atomic photoionization cross sections, so that the observed intensity should represent the total density of states weighted by the appropriate photoionization cross sections, i.e.,

$$I(E_f,\hbar\omega) \propto \sum_i |\sigma_i(\vec{k}_f)|^2 \delta(E_f - E_i - \hbar\omega) , \quad (26)$$

where the summation extends over all initial states in the Brillouin zone. The photoionization cross sections ought to exhibit an angular dependence since the local symmetry of the final-state wave function in the region of the core is not altered much by the phonon disorder. (However, the thermal disorder might alter the hybridization of the final state so that the weighting of various states is changed.) In the limit of extreme disorder, $\sigma_i(k_f)$ should be strictly the atomic photoionization cross section.

McFeely *et al.*[3] have suggested that orbital projections of the density of states ought to be observed when the acceptance angle of the electron velocity analyzer is large enough to collect contributions from all initial states in the Brillouin zone. However, phonon disorder can allow such orbital projections to be observed in the limit in which the acceptance angle is zero.

The magnitude of the thermal displacements at room temperature for atoms in several solids, as calculated by Eq. (23) and listed in Table I, are on the order of 0.1 Å. Low-energy diffraction mea-

TABLE I. Tabulation of the thermal displacements U_0^2 at room temperature for several elements as given by Eq. (23). Also included is the contribution to the energy width, ΔE, [see Eq. (A8) due to thermal vibrations at room temperature for final states with kinetic energies of 1500 eV]. The Debye temperatures are taken from Ref. 19.

Element	Θ_m (°K)	U_0^2 (Å^2)	ΔE (meV)
Cu	320	0.0067	54
Ag	210	0.0100	40
Au	175	0.0071	30
Tl	93	0.0170	29
Be	900	0.0054	143
Mg	320	0.0177	90
Ca	230	0.0210	68
Al	390	0.0106	83
Sn	130	0.0211	40
Ta	245	0.0040	32
Bi	100	0.0216	30
Pb	88	0.0270	29
Cr	485	0.0037	59
Mo	380	0.0031	44
W	310	0.0025	32
Fe	430	0.0043	58
Co	410	0.0044	56
Ni	400	0.0040	56
Pd	275	0.0054	42
Ir	285	0.0027	31
Pt	230	0.0040	31

surements indicate that the thermal displacements of the atoms in the first 1–4 layers might be twice those of the bulk.[20-21] Therefore, the effects of thermal disorder become even more important as the surface sensitivity of the photoemission experiment is increased.

According to Eq. (25), the thermal disorder is not very important for ultraviolet photons where $k_f < 5$ Å^{-1}, but it almost totally destroys k conservation in the XPS regimes, where $k_f \sim 20$ Å^{-1}. Since the relative displacements of nearest-neighbor atoms is half of that of atoms far apart, the x-ray spectra still might exhibit nearest-neighbor interferences, but not much more. We therefore challenge the validity of several recent models in which k conservation has been assumed to be applicable in the XPS regime at room temperature.[1-4] Effects due to band-structure dispersion should not be observed in the XPS regime, unless the sample is cooled sufficiently to reduce the magnitude of thermal vibrations. We also suggest that increasing the temperature might allow orbital projections of the density of states to be determined at lower photon energies.

In the case of photoemission from layered materials, the thermal displacements between the weakly bound layers is large (~0.3 Å), and therefore, the destruction of the component of the momentum perpendicular to the layers might be significant for final-state energies in the UPS regime. The photoemission[22] and optical spectra[23] of Bi show a strong temperature dependence. Recent angle-resolved photoemission spectra for $h\nu = 16.9$ eV look much like one-dimensional densities of states,[24] which might be due to the fact that the Debye temperature of Bi is ~100 K.

We also suggest that thermal vibrations might destroy interferences between weakly bound adsorbates and the underlying substrate surface for low final-state energies. Only the internal structure of the adsorbates ought to contribute to the angular variations.

It has been noted that as the final-state energy increases, the angle-averaged photoemission spectra lose structure due to k conservation and begin to look more like the total density of states.[10] This transition from bandlike behavior to density-of-states-like behavior, called the "XPS limit," has been attributed to two possible mechanisms: (i) The increasing number of final-state bands, and (ii) the finite mean-free path of the photoelectron. Mechanism (i) can bring about the XPS limit for $h\nu \sim 40$–100 eV, where the mean-free path of the photoelectron is 2–5 Å, but for $h\nu \sim 1500$ eV where the mean-free path is 20–50 Å, this mechanism cannot be important.[10] One would thus expect mechanism (i) to bring about the "XPS limit" at large photon energies. However, it is clear that phonon disorder can bring about this limit even when few final-state bands are available. While mechanisms (i) and (ii) predict the angle-resolved spectra at high photon energies to resemble the one-dimensional density of states, the phonon-disorder mechanism predicts that they will resemble the orbital projections of the total density of states.

Not only can phonon disorder bring on the destruction of the electronic k conservation and the "XPS limit", but it can also cause a noticeable smearing in energy of the spectra as higher-order phonon processes make an appreciable contribution. While the first-order processes relax the energy-conservation constraint by $\pm k\Theta_m$; processes of order n should cause a smearing n times this amount. For most of the materials listed in Table I, the second-order processes are likely in the XPS regime ($h\nu \sim 1500$ eV), and therefore, the energy smearing due to phonon-aided optical transitions is 0.2 eV. Cooling of the sample should not only restore k conservation, but the spectra should sharpen in energy as well. It would be of interest to determine the shape of the Fermi edge as a function of temperature in a high-resolution XPS experiment to see whether it shows the broadening effects of phonon-induced transitions.

IV. COMPOSITIONAL DISORDER

In this section, we consider the effects of compositional disorder for which two or more types of atoms are randomly distributed upon a crystalline lattice. We consider the case in which k is still a valid quantum number for the initial state. This might occur, for example, in Si-Ge alloys where the pseudopotentials of Ge and Si are nearly similar.[25] (However, in other cases, such as Cu-Ni alloys, the d orbitals of the two atoms lie at different energies, and therefore, k is not expected to be a valid quantum number.[26]) The photoionization transition probability for an alloy takes the form

$$|M_{fi}|^2 = \sum_{m,n} \sigma_m \sigma_n^* \exp[i\Delta\vec{k} \cdot (\vec{R}_m - \vec{R}_n)]. \qquad (27)$$

To evaluate this sum, it is necessary that the correlations between the various types of elements be known. Angle-resolved photoemission spectroscopy, therefore, might allow the types of correlations between the different kinds of atoms to be determined, in a manner similar to that employed with x-ray diffraction.[18,19] However, an advantage of photoemission is that the relative sizes of the σ_i's can be varied over a wide range by changing the photon energy, allowing the sensitivity to par-

ticular correlations to be altered.

When all of the matrix elements are the same, the sum in Eq. (27) can be evaluated to show that k-conserving transitions dominate the spectra and strong angular variations are expected. When the atoms are randomly distributed on the sites with uniform probabilities, the total cross section takes the form

$$|M_{fi}|^2 = \sum_{m,n} (\bar{\sigma} + \Delta\sigma_m)(\bar{\sigma}^* + \Delta\sigma_n^*) \exp[i\Delta\vec{k} \cdot (\vec{R}_m - \vec{R}_n)]$$

$$= (\bar{\sigma})^2 \sum_G \delta(\Delta\vec{k} - \vec{G}) + \Delta\bar{\sigma}^2 , \tag{28}$$

where

$$\Delta\sigma_m = \sigma_m - \bar{\sigma} ,$$

$$\bar{\sigma} = \sum_m c_m \sigma_m ,$$

$$\bar{\sigma}^2 = \sum_m c_m |\sigma_m|^2 ,$$

$$\Delta\bar{\sigma}^2 = \Delta\sigma^2 = \bar{\sigma}^2 - |\bar{\sigma}|^2 ,$$

and c_m is the concentration of atom m. For a photon energy in which only atom of type p has a nonvanishing cross section, the cross section becomes

$$|M_{fi}|^2 \cong c_p^2 |\sigma_p|^2 \sum_G \delta(\Delta\vec{k} - \vec{G}) + (c_p - c_p^2) |\sigma_p|^2 . \tag{29}$$

The k-conserving transitions vary as the square of the concentration, while those involving indirect transitions behave linearly with the concentration. For dilute concentrations of atom p, the spectra ought to reveal the local density of states about the atom modulated by the atomic-like photoionization cross sections for all final-state energies, including the UPS regime. If there are many tendencies for the atoms having a large cross section to cluster together, interference effects, i.e., k conservation should still be present in the spectra.

V. LONG-RANGE POSITIONAL DISORDER

In the presence of long-range positional disorder, such as that occurring in liquids and amorphous solids, the k vector is not a good quantum number for the initial state.[12] In general we might write for the initial state

$$\psi = \sum_m a_m \phi_m(\vec{r} - \vec{R}_m) , \tag{30}$$

where the phase of a_m varies in some manner from site to site, but the amplitude does not. Also, the nature or orientation of the atomic orbitals, ϕ_m, must vary from site to site. Assuming that the APW still describes the final state, we obtain for the photoionization cross section

$$|M_{fi}|^2 = \sum_{mn} \langle a_m^* a_n \rangle \sigma_m^* \sigma_n \exp[i\vec{k}_f \cdot (\vec{R}_m - \vec{R}_n)] . \tag{31}$$

It might be reasonable to assume that the concept of a k vector at least describes the local phase variation of the electron state. However, since the system is isotropic on the average, a reasonable phase correlation function might have the form

$$\langle a_m a_n^* \rangle = \langle \exp(i\vec{k} \cdot \vec{r}_{mn}) \rangle = \sin(kr_{mn})/kr_{mn} , \tag{32}$$

where k is the local momentum. With this ansatz, the structure factor becomes

$$\frac{S(\Delta k)}{N} = 1 + \int_0^\infty 4\pi r [\rho(r) - \rho_0] \frac{\sin(k_i r)}{k_i r} \times \frac{\sin(k_f r)}{k_f r} \, dr , \tag{33}$$

where $\rho(r)$ is the atomic pair-pair correlation function and ρ_0 is the average atomic density.[18,19] For initial states with $k_i = 0$, the integral is equivalent to the x-ray interference function.

Diffraction studies have shown that the $S(k)$ of liquids and amorphous solids has spherically isotropic diffuse diffraction peaks which rapidly decay for $k > 5$ Å^{-1}.[18,19] Therefore, angular variations in the spectra due to interference effects are not expected, but interference effects might occur which depend upon the magnitude of the final-state momentum. Assuming the nearest-neighbor shells to be distributed according to Gaussian functions,[27] the structure factor for $k_i = 0$ becomes

$$\frac{S(k)}{N} = 1 + \sum_i \frac{c_i}{kr_i} e^{-k^2 w_i^2} \sin(kr_i) \tag{34}$$

where w_i, r_i, and c_i are the static spread, position, and coordination number of shell i, respectively. For most disordered solids, $w_2 \sim 0.5$ Å^{-1}, and thus interferences between second neighbors becomes small for $k_f \sim 3$ Å^{-1}. In many cases, where the nearest-neighbor shell is as sharply defined as in the crystalline materials, the initial states having $k_i = 0$ should exhibit weak interference extended x-ray-absorption fine structure (EXAFS) effects resembling oscillations as a function of the photon energy for final-state energies extending into the XPS regime.[28] Such oscillations should be much weaker as the reduced momentum of the initial state increases, as can be seen in Eq. (33).

It appears that the disorder in liquids and amorphous solids is sufficient to bring about the XPS limit for very small final-state energies. Low-energy photoemission experiments on amorphous materials have indeed demonstrated that the spectra appear to reveal the density of states even at the onset of photoemission.[29]

VI. DISORDER AND THE SURFACE TRANSPORT STEP

So far, we have considered only the effects of disorder upon the optical excitation step of the photoemission process. However, we must also consider how the electron state inside of the bulk is modified as it passes through the surface into the vacuum. To explain such effects, one must investigate the matching at the surface of the final state inside of the solid to the free-electron waves outside of the solid.[9,10,30]

Let us consider the boundary of the solid to lay in the x-y plane and to be characterized by a potential change by the amount W (the inner potential). Assuming that the electron state outside of the solid has a Fourier expansion

$$\psi_0 = \int a_k e^{i\vec{k}\cdot\vec{r}}\,\delta(|k| - \sqrt{E})\,d^3k\,, \tag{35}$$

we find that in order for the solution outside to be continuous at the boundary to the state, $\psi_i(r)$, inside of the solid,

$$a_k = \int e^{-i\vec{k}\cdot\vec{r}}\,\psi_i(r)\,dS\,, \tag{36}$$

where the integration is performed over the boundary plane. (We presently ignore the requirement of continuity of the derivative at the boundary, since we are concerned about only the qualitative effects of disorder.)

Now we consider the effects of the surface disorder on an internal state consisting of a single plane wave with a wave vector k_i. In the absence of disorder, Eq. (36) yields the result[9,10]

$$a_k = \delta(k_\parallel - k_{i\parallel})\,, \tag{37}$$

which is the usual conservation of the component of momentum parallel to the surface.[9,10]

We introduce a fluctuation in the position of the surface in the z direction by the amount

$$\Delta z = \int \zeta(\vec{\xi})e^{i\vec{\xi}\cdot\vec{r}_\parallel}\,d^2\xi\,, \tag{38}$$

where $r_\parallel$ is the position coordinate in the unperturbed surface plane. Inserting (38) into (36) and performing an ensemble average over the phases of $\zeta(\xi)$, we obtain

$$|a_k|^2 = \int \exp[i\Delta\vec{k}_\parallel\cdot\vec{r}_\parallel - (\Delta k_\perp^2)U_s^2\gamma_s(r_\parallel)]\,d^2r_\parallel\,, \tag{39}$$

where

$$U_s^2 = \int |\zeta(\vec{\xi})|^2 d^2\xi\,, \tag{40}$$

$$\gamma_s(r_\parallel) = 1 - \frac{1}{U_s^2}\int |\zeta(\vec{\xi})|^2 e^{i\vec{\xi}\cdot\vec{r}_\parallel} d^2\xi\,, \tag{41}$$

and $\Delta k_\parallel$ and $\Delta k_\perp$ are the differences in the components of the wave vectors of the internal and external plane waves parallel and perpendicular to the solid. The quantity U_s^2 is the average square of the surface fluctuations, and $\gamma_s(r)$ is the correlation function for the surface fluctuations. For an isotropic surface roughness,

$$\gamma_s(r) = 1 - \frac{2}{\pi U_s^2}\int_0^\infty |\zeta(\vec{\xi})|^2 J_0(\xi r)\xi\,d\xi\,, \tag{42}$$

where J_0 is the zero-order Bessel function. In the case where γ_s is unity for $r > L$ and zero for $r < L$, Eq. (39) yields

$$|a_k|^2 = (1 - e^{-\Delta k_\perp^2 U_s^2})\int_0^L e^{i\vec{\Delta}k_\parallel\cdot\vec{r}_\parallel} d^2r_\parallel + e^{-\Delta k_\perp^2 U_s^2}\delta(\Delta\vec{k}_\parallel)\,. \tag{43}$$

The first term in Eq. (43) corresponds to a breakdown of $k_\parallel$ conservation across the surface by the amount $\Delta k = 1/L$. It is necessary for L to be on the order of an interatomic spacing for the momentum conservation to be broken down noticeably. The second term in Eq. (43) corresponds to the maintenance of perfect k conservation parallel to surface, which is similar to the result found for the photoionization cross section. However, in the present case, the breakdown of k conservation depends upon the *differences* of momentum between the final state inside and outside of the surface.

When the solution inside of the solid is a single plane wave, the difference in the component of momentum perpendicular to the surface is

$$\Delta k_\perp = k_\perp - (k_\perp^2 + 2mW/\hbar^2)^{1/2}\,, \tag{44}$$

where $k_\perp$ is the wave-vector component of the electron state outside of the solid. As $k_\perp$ increases, the difference in momenta decreases, and thus, the effects of the surface disorder in destroying k conservation becomes less important. For the free-electron state, the effects of the disorder are most important near threshold or large emission angles where $\Delta k_\perp = (2mW/\hbar^2)^{1/2}$. In these cases, the states that normally cannot escape from a perfect surface due to the refraction effects, can now couple to external propagating states. The spectra near the work-function cutoff should not necessarily decrease with energy as it does for a perfect surface, but might actually increase as the electron energy decreases. We therefore suggest that the shape of the cutoff tail provides a sensitive test for the degree of smoothness of the surface.

Although the sensitivity of the spectra to surface roughness decreases with final-state energy when the states are plane waves, it cannot decrease at higher energies when the increasing number of bands is responsible for bringing on the "XPS limit"

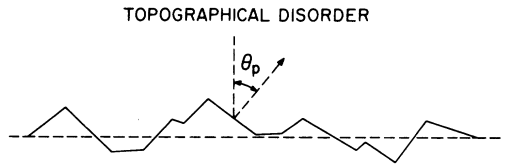

FIG. 2. Schematic representation of a topographically disordered surface. The dotted line corresponds to the ideal surface plane and θ_p is the angle that the defect plane makes with respect to the ideal plane.

(i.e., mechanism (i) discussed in Sec. III). When there are several final states occurring along any direction in the Brillouin at a given energy, some of the states must have a wave vector that deviates from the free wave vector outside by as much the width of the Brillouin zone.

Since the surface matching condition depends upon the difference of the wave vector of the wave function inside and outside of the solid, rather than the absolute value of the final-state wave vector, phonon disorder is not large enough to destroy k conservation at the surface for any final-state energy. However, if roughness on the order of atomic dimensions is introduced to the surface, such as by impurities and adsorbates, the surface k conservation should be weakened even in the XPS regime. When the surface k conservation condition is relaxed, the spectra should lose the angular variations, and they ought to reflect the angle-averaged spectra associated with the face of emission. Since the correspondence between the momentum inside and outside of the solid is lost, orbital projections of the density of states, as was discussed in Sec. III, are not expected to be observed.

VII. SURFACE REFRACTION AND TOPOGRAPHICAL DISORDER

In this section, we consider the influence of topographically disordered surfaces on the angle-resolved photoemission spectra. As is shown in Fig. 2, such a surface consists of several smaller defect planes which are smooth on a microscopic scale (~100 Å), but which are no longer parallel to the perfect surface plane. Although the orientation of the surface plane is disordered, the underlying crystallographic order of the atoms might be unaltered. Topographically disordered surfaces are usually formed when the sample is subjected to ion bombardment and the interstitials and vacancies are mobile.[31]

As long as the planes have dimensions of a few tens of angstroms, the correlations in positions between the planes can be neglected and the emission from each plane can be treated separately.

In order to determine the importance of topographical disorder, we must consider the angle of refraction of the photoelectron at the surface planes. The continuity condition requires that the component of momentum parallel to the surface be conserved as the photoelectron passes through the surface. The change in the angle of propagation arises from a change in the component of momentum perpendicular to the surface. Using the fact that the angle of propagation with respect to the crystal surface is

$$\sin\theta = k_{\parallel}/(k_{\parallel}^2 + k_{\perp}^2)^{1/2}, \tag{45}$$

where $k_{\perp}$ and $k_{\parallel}$ are the components of the wave vector perpendicular and parallel to the surface, it can be shown by differentiation that the change in angle due to the change in $k_{\perp}$ is

$$d\theta \cong \sin\theta \, \frac{dk_{\perp}}{k_0}, \tag{46}$$

where k_0 is the magnitude of the momentum of the photoelectron. In the case where the electrons are free wave-like inside and outside of the solid and the surface boundary is described by a jump in the potential of amount W [see Eq. (44)], the change in perpendicular component of momentum to first order in W is

$$dk_{\perp} \cong \frac{W}{2k_{\perp}} = \frac{W}{2k_0\cos\theta}. \tag{47}$$

Inserting this into Eq. (46), we find that

$$d\theta \cong \frac{1}{2}\,\frac{W}{E_0}\tan\theta, \tag{48}$$

where E_0 is the kinetic energy of the photoelectron. In the free-electron case, the importance of refraction diminishes quickly as the kinetic increases. For $E_0 = 100$ eV, $W = 10$ eV, $\theta \sim 30^0$, $d\theta \cong 3^0$. In XPS regime the refraction effects of free electrons is negligible. This well-known fact has led some workers to ignore refraction effects for $h\nu \gtrsim 100$ eV. However, if the density of final bands increases with photon energy, then as discussed in Sec. VI, there are always final states for which the difference in their momentum inside of the solid and that of the free-electron state outside is the width of the Brillouin zone, G_0. For such states, the refraction angle is

$$d\theta \cong \frac{G_0}{k_0}\sin\theta. \tag{49}$$

The importance of refraction for these states decreases more slowly with the final-state energy than for the free-electron case. For example in Cu, $G_0 \cong 2.5$ Å^{-1}. For $\theta \sim 30^0$, $h\nu = 100$ eV, $d\theta \cong 15^0$! For the XPS regime $d\theta \cong 3^0$. The above estimates are for the worst cases, but on the average, they

should be about half of this amount. Thus, it is clear that when the final states become distributed throughout the Brillouin zone, the effects of refraction cannot be neglected even in the XPS regime. The differences in the spectra observed along a crystallographic axis perpendicular to the surface and spectra observed for an equivalent axis that is not perpendicular to the surface might be explained by non-negligible refraction effects.

In the presence of topographical disorder, the average uncertainty in the internal angle of propagation of the states inside of the solid emerging into final states propagating along the crystallographic axis normal to macroscopic surface is for the free-electron case,

$$\langle\theta_e\rangle = \frac{1}{2}\frac{W}{E_0}\int_0^{\pi/2} \tan\theta\cos\theta\, P(\theta)\, d\theta \tag{50}$$

where $P(\theta)$ is the probability that a plane makes an angle θ with respect to axis of emission. The $\cos\theta$ factor comes from the escape probability due to the finite mean-free path of the photoelectron.

For small deviations of the surface defect planes from the macroscopic plane, Eqs. (47) and (50) yield

$$\langle\theta_e\rangle = \tfrac{1}{2}(W/E_0)\langle\theta_p\rangle\,, \tag{51}$$

where $\langle\theta_p\rangle$ is the average angle that the defect surface planes make with respect to the macroscopic plane.

When the density of final-state bands is large, Eqs. (49) and (50) yield

$$\langle\theta_e\rangle = (G_0/2k_0)\langle\theta_p\rangle\,. \tag{51}$$

When the topographical disorder is large, the angle-resolved photoemission spectra are expected to exhibit a weak angular dependence. For certain polar and azimuthal angles, many of the defect surfaces might be shadowed so that only a few of them contribute, making the structure in the spectra more sharply defined than for emission normal to the macroscopic surface, where more defect planes are likely to contribute. As the photon energy increases, the effects of the topographical disorder become weaker when the states are free-electron-like. However, when several final states contribute to the photoemission spectra and Eq. (49) is valid, the uncertainty in the momentum due to topographical disorder remains constant with photon energy, its magnitude being equal to $\pm\langle\theta_p\rangle G_0$.

The topographical disorder ought to be most severe in altering the angular variations in the spectra from adsorbates on the surface, for which the orientation of the surface plane is critical for aligning the molecular orbital states. For this case, the effects of the topographical disorder will not decrease as the final-state energy increases, the average uncertainty in the emission angle remaining equal to $\langle\theta_p\rangle$. The presence of topographical disorder might be detected by observing the degree to which emission from surface overlayers is enhanced at large polar angles. For a perfectly smooth surface, the enhancement ought to be strong, but for a topographically disordered surface, the enhancement ought to be weak.

VIII. DIRECTED PHOTOEMISSION–A TEST FOR THE MODELS

In this section, we show that photoemission spectra directed along a crystallographic axis provide the crucial test for determining which of the proposed models for the final state is valid. The description of the emission directed along a low-index crystallographic axis is simplified greatly by the symmetry associated with that axis.

When the acceptance aperture of the electron velocity analyzer is positioned along a particular axis, it detects an electron state outside of the solid which has the form $e^{ik_f z}$, where z is directed along the symmetry axis. This function is purely symmetric with respect to rotations about the symmetry axis and to reflections through mirror planes passing through the symmetry axis. By continuity the wave function inside of the solid must have the same symmetry. The state that is even with respect to all symmetry operations about the crystallographic axis of emission always is contained in a group in which the characters are all unity.[14] Since the plane-wave functions of the form e^{ikz} fall entirely into this group, they cannot be contained in wave functions of different symmetry and, therefore, final states of other symmetries cannot be detected along the axis of emission. This constraint also applies to photoemission from adsorbed molecules. When the wave function inside of the solid is expressed in terms of a plane-wave expansion

$$\phi_{nk} = e^{i\vec{k}\cdot\vec{r}}\sum_G U_{nk}(\vec{G})e^{i\vec{G}\cdot\vec{r}}, \tag{52}$$

the matrix element connecting the initial and final state is

$$M_{fi} = \sum_G \vec{A}\cdot\vec{G}\, U^*_{n_f k_f}(\vec{G})U_{n_i k_i}(\vec{G})\,, \tag{53}$$

where $\vec{A}$ is the vector potential.

From Eq. (53), it can be seen that a final state in the solid consisting of a single plane wave can couple, via the dipole operator, only to the initial states which contain this plane wave. Such initial states must also be purely symmetric with respect to the symmetry operations associated with the

crystallographic axis. We suggest that when k conservation is valid, the strength of emission from initial states of symmetry different from that of the purely symmetric states provides a measure of the failure of the plane-wave final state.

It has been suggested in Sec. II that a single APW provides additional improvements to the plane-wave final state, since it restores the validity of the atomic dipole selection rules. The spherical waves contained in the APW are those for which $m=0$ relative to the z axis. Although initial states that are derived from orbitals with $m=0, \pm 1$ can be photoexcited, initial states derived from orbitals with $m \geq 2$ cannot couple to the single APW final state. Since the optical excitation step takes place via APW's components propagating in directions other than the emission axis, while the escape step occurs via the component propagating along the emission axis, the initial states with $m \geq 2$ can appear in the photoemission spectra only if the APW's are mixed among themselves. Therefore, we suggest that the strength of emission from the states with $m \geq 2$ compared to the emission from states with $m \leq 1$ indicates the amount by which the APW states are mixed. Modulations in the strength of emission of the initial states with $m \geq 2$ relative to those with $m \leq 1$ might occur as the degree of hybridization of the final state changes with photon energy.

An additional difficulty of the single APW as expressed in Eq. (4) is that it predicts modulations in the absorption coefficient from core levels which are nearly 100% (since for some final-state energy, $j_l(ka)=0$) while the observed modulations are only 10%.[29] This problem could be removed if the derivative of the APW wave function were made continuous at the muffin-tin radius.

As mentioned, at higher final-state energy, the plane-wave part of the APW provides the dominant channel for the escape process. One might, therefore, conclude that the emission directed along any one axis ought to be dominated by that single APW propagating in this direction, and that only one initial state along the axis of emission contributes to the spectra. However, single APW's propagating in other directions have reduced k vectors that are also directed along the axis of emission, as is illustrated in Fig. 3. The magnitude of the reduced k vectors directed along the axis of emission are found by the set of shortest vectors connecting the reciprocal-lattice points with the free-wave sphere of radius k_f. Although the primary component of these final states is not directed along the axis of emission, some of their secondary ones are. The secondary cones come from the core part of the APW and are of order λ (see Sec. II) relative to the plane-wave portion of the

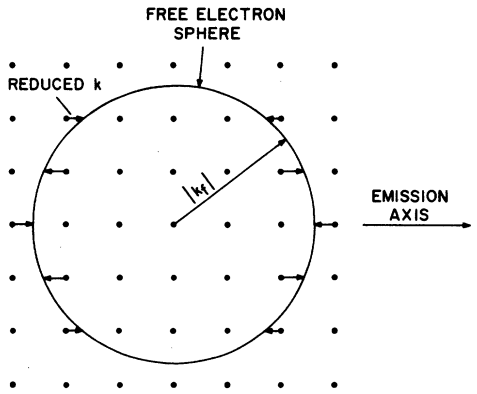

FIG. 3. Construction for finding the reduced k values of free-electron waves along the crystallographic axis indicated.

APW. Although the secondary plane waves might be small, there are many of them contributing along the axis of emission; consequently, the emission from secondary components might actually be larger than from the primary ones. In fact, when a single APW provides a valid description for the final state, the $m \geq 2$ initial states can escape by the secondary components only. The total strength of the secondary emission relative to the primary emission is roughly given by

$$\Gamma = \lambda N_f , \tag{54}$$

where N_f is the total number of free-electron states that have a reduced momentum lying along the axis of emission. The number of such states is given by the volume of a shell in k space of radius k_f and thickness G_0, the radius of the Brillouin zone, divided by the volume of the Brillouin zone or,

$$N_f \cong \frac{4\pi k_f^2 G_0}{\frac{4}{3}\pi (G_0)^3} = \frac{3k_f^2}{G_0^2} . \tag{55}$$

Thus, in order for the spectra of electrons directed along a particular axis to be dominated at high photon energies by a single point in k space, it is necessary that λ decrease faster than the kinetic energy of the final electron state. For an atomic potential varying as r^{-n}, it can be shown that

$$\Gamma \propto T_f^{1-3/n} . \tag{56}$$

Provided that $n < 3$, the secondary emission become less important as the kinetic energy of the final state, T_f, increases.

Finally, in Fig. 4, we have sketched the form of the spectra directed along the [111] axis from the d electrons in Ag for various final-state models. In Fig. 4(a) we have plotted the density of states

associated with the (111) direction taken from the band structure of Smith.[32] The upper two peaks are from Λ_3 bands derived primarily from d orbitals with $m = \pm 1$, the next two peaks (3 and 4) with $m = \pm 2$, and the last peak (5) from a Λ_1 band, with $m = 0$. The single plane-wave final state predicts that a state with $m = 0$ from only one point in k space ought to appear in the spectra, as is indicated in Fig. 1(b). Initial states with $|m| > 0$ have a vanishing charge density in the direction of propagation, and consequently, they do not appear in the spectra. For final states consisting of an APW, only a single point in k space with states having $m = 0, \pm 1$ are allowed to contribute, and the states having $m = \pm 2$ are forbidden [see Fig. 4(c)]. When the APW waves are strongly hybridized, not only are the $m = 2$ states allowed, but more than one final state along the axis of propagation must necessarily contribute to the spectra; the spectra, therefore, ought to resemble the one-dimensional density of states associated with the [111] axis, as is shown in Fig. 4(a). When phonon disorder is introduced the spectra ought to resemble projections of the total density of states, the angular behavior of the atomic cross sections depending upon the nature of the final state [Fig. 4(d)]: For the plane-wave state, it is the momentum projection along the [111] axis; for the APW, it is the projection of atomic orbitals for which $|m| \leq 1$; and for the hybridized APW, it should more or less resemble the total density of states.

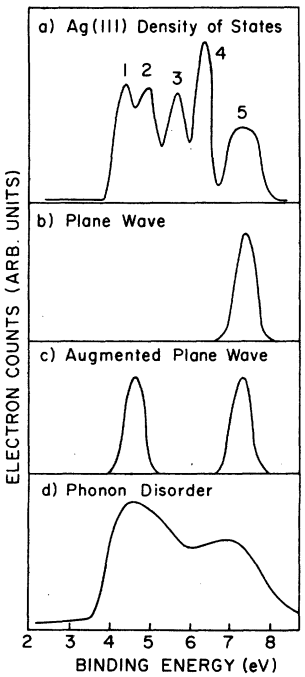

FIG. 4. (a) One-dimensional density of states along the [111] axis of Ag. The photoemission spectra along the [111] axis of Ag predicted for (b) a plane-wave final state, (c) an Augmented plane-wave final state, and (d) for phonon disorder.

Recent photoemission experiments on the noble metals seem to indicate that the initial states for $m \geq 2$ appear with strengths similar to the initial states for $m \leq 1$.[1-5,7] However, the acceptance angle of the analyzer in these experiments was sufficiently large so that all states in the Brillouin zone could contribute, even if k were conserved. The symmetry restrictions considered here are no longer valid when states lying off of the symmetry axis contribute significantly to the photoemission spectra. Experiments performed with a smaller angle of acceptance and as a function of temperature appear to be necessary to sort out the relevance of k conservation and the nature of the final electron state.

IX. SUMMARY AND CONCLUSIONS

In this paper, we have considered the nature of the final electron state, and the influence of bulk and surface disorder upon the angle resolved photoelectron spectra.

It has been argued that a plane-wave final state is inadequate for describing the optical ionization step of the photoemission process since it improperly describes the spherical symmetry of the true final state in the vicinity of the electron core. By employing an augmented plane-wave final state, we found that the interferences between the atoms are still those obtained with a plane-wave final state, but that the photoionization cross sections are governed by atomic dipole selection rules.

The influence of phonon disorder is not expected to be very important in the UPS regime at room temperature, but in the XPS regime, it is sufficient to destroy k conservation completely and to bring about the "XPS limit" in which the spectra resemble density of states. Compositional and long-range disorder are usually sufficient to destroy k conservation in the UPS regime.

Surface roughness on an atomic scale, such as that induced by impurities, adsorbates, and surface vacancies, can cause a breakdown of the conservation of the component of the momentum parallel to the surface. When the number of final states contributing to the spectra increases with photon energy, the influence of surface roughness is not diminished. The portion of the spectra closest to the work-function cutoff is expected to be the most sensitive to surface roughness, and therefore its shape should provide a useful test for the condition of the surface.

Topographical disorder can also smear the angle

dependence of the photoemission spectra when the refraction of the electron at the surface is important.

Finally, it was argued that the photoelectron spectra directed along low-index crystallographic axis provide a good test for the validity of several final-state models, owing to the symmetry associated with that axis. It is suggested that such experiments be performed with a small acceptance angle and at low temperatures to remove the phonon disorder.

Since this paper has been submitted for publication, Williams *et al.*,[33] have found that the photoemission spectra of Cu at 50 eV show a pronounced weakening of k conservation effects as the temperature increases, in general agreement with the results predicted here.

The primary message of this paper has been that theories developed for ideal situations cannot be applied to real experimental spectra unless the effects of disorder are taken into account. If this is not done, the field of angle-resolved photoelectron spectroscopy is likely to lapse into a state of disorder itself.

ACKNOWLEDGMENTS

Conversations with S. Kirkpatrick, N. V. Smith, J. Herbst, J. Gadzuk, and D. Leibowitz are gratefully acknowedged.

APPENDIX A: THERMAL VIBRATIONS AND ENERGY CONSERVATION

The first term in Eq. (25) gives the total number of transitions which have taken place via interactions with phonons. However, in the derivation of Eq. (25), the time variation in the relative displacements of the atoms has been ignored. In this Appendix, we include such displacements and extend the simple Debye model to include the effects of energy conservation.

Retaining the time dependence of the terms for which $n=m$ in Eqs. (15) and (16), we find that the time-dependent equivalent of Eq. (25) is

$$S(\Delta k, t) = N\{\exp\{-\Delta k^2 U_0^2[1-\Gamma(t)]\} - \exp(-\Delta k^2 U_0^2)\} + \exp(-\Delta k^2 U_0^2)\sum_G \delta(\Delta\vec{k}-\vec{G}), \quad \text{(A1)}$$

where

$$\Gamma(t) = \frac{\sum_{qj}|a_{qj}|^2(\vec{\epsilon}_{qj}\cdot\vec{\epsilon}_{\Delta k})^2\cos\omega_{qj}t}{\sum|a_{qj}|^2(\vec{\epsilon}_{qj}\cdot\vec{\epsilon}_{\Delta k})^2}. \quad \text{(A2)}$$

In the limit that $\Delta k U_0 \gg 1$, i.e., most of the optical transitions are of a thermal diffuse nature, the time-dependent exponential in (A1) decays very rapidly, and it can be approximated with the small time behavior of $\Gamma(t)$ to yield

$$S(\Delta k, t) = N\exp(-\Delta k^2 U_0^2\langle\omega_q^2\rangle t^2). \quad \text{(A3)}$$

The Fourier transform of (A3) with respect to time is

$$\frac{S(\Delta k, \omega_s)}{N} = \frac{\exp[-\omega_s^2/2(\Delta k U_0)^2\langle\omega_q^2\rangle]}{[2\pi(\Delta k U_0)^2\langle\omega_q^2\rangle]^{1/2}}. \quad \text{(A4)}$$

This function gives the distribution of energy which the lattice contributes to optical excitation process. The width of this Gaussian function at half-maximum is

$$\Delta\omega = (\ln 2)^{1/2} 2\Delta k U_0(\langle\omega_q^2\rangle)^{1/2}. \quad \text{(A5)}$$

For the case in which the phonons have the same velocity it is trivial to show that $\langle\omega_q^2\rangle = \frac{1}{3}\omega_m^2$, where ω_m is the maximum phonon frequency, and (A5) becomes

$$\Delta\omega = 2(\tfrac{1}{3}\ln 2)^{1/2}\Delta k U_0\omega_m. \quad \text{(A6)}$$

In terms of the energy width this can also be written as

$$\Delta E = 2(\tfrac{1}{3}\ln 2)^{1/2}\Delta k U_0 k_B\Theta_m. \quad \text{(A7)}$$

Using Eq. (23), the energy width becomes

$$\Delta E = 2\hbar\Delta k[(\ln 2)k_B T/M_A]^{1/2}. \quad \text{(A8)}$$

The only material dependent quantity upon which the energy width depends is the mass of the atom. In fact, we recognize that expression (A8) is very close to what we would have obtained if we considered the uncertainty in the velocity of the initial electron to be that of the atom to which it is bound.

*Work supported by the NSF (DMR-75-21867).

[1]P. S. Wehner, J. Stohr, G. Apai, F. R. McFeely, and D. A. Shirley, Phys. Rev. Lett. 38, 169 (1977).
[2]L. F. Wagner, Z. Hussain, and C. S. Fadley, Solid State Commun. 21, 257 (1977).
[3]F. R. McFeely, J. Stohr, G. Apai, P. S. Wehner, and D. A. Shirley, Phys. Rev. B 14, 3273 (1976).
[4]R. J. Baird, L. F. Wagner, and C. S. Fadley, Phys. Rev. Lett. 37, 111 (1976).
[5]J. Stohr, G. Apai, P. S. Wehner, F. R. McFeely, R. S. Williams, and D. A. Shirley, Phys. Rev. B 14, 5144 (1976).
[6]P. M. Williams, P. Butcher, and J. Wood, Phys. Rev. B 14, 2215 (1976).
[7]N. J. Shevchik and D. Liebowitz, Phys. Rev. (to be published).
[8]R. Stanley Williams and D. A. Shirley, J. Chem. Phys. 66, 2378 (1974).

[9]G. D. Mahan, Phys. Rev. B 2, 4334 (1970).
[10]P. J. Feibelman and D. E. Eastman, Phys. Rev. B 10, 4932 (1974).
[11]J. W. Gadzuk, Phys. Rev. B 10, 5030 (1974).
[12]D. Weaire and M. F. Thorpe, Phys. Rev. B 4, 3518 (1971).
[13]J. M. Ziman, *Electrons and Phonons* (Oxford U.P., London, 1960).
[14]J. Callaway, *Energy Band Theory* (Academic, New York, 1964).
[15]U. Fano and J. W. Cooper, Rev. Mod. Phys. 40, 441 (1968).
[16]J. W. Rabalais and T. P. Debies, J. Electron Spectrosc. Relat. Phenom. 5, 847 (1974).
[17]J. F. Herbst, Phys. Rev. B 15, 3720 (1977).
[18]B. E. Warren, *X-ray Diffraction* (Addison-Wesley, Reading, Mass., 1964).
[19]R. W. James, *The Optical Principles of the Diffraction of X-rays* (Cornell University, Ithaca, 1965).
[20]R. J. Reid, Surf. Sci. 29, 623 (1972).
[21]G. E. Laramore and C. B. Duke, Phys. Rev. B 2, 4783 (1970).
[22]G. J. Lapeyre, T. Huen, F. Wooten, Solid State Commun. 8, 1233 (1970).
[23]M. Cardona and D. L. Greenaway, Phys. Rev. 133, A1685 (1964).
[24]D. Liebowitz, J. Muratore, Y. H. Kao and N. J. Shevchik, Solid State Commun. 22, 759 (1977).
[25]D. Stroud and H. Ehrenreich, *Proceedings of the Tenth International Conference on the Physics of Semiconductors*, edited by S. P. Keller, J. C. Hensel, and F. Stern (U.S. AEC Div. Tech. Information, Oak Ridge, Tenn., 1970), p. 652.
[26]S. Velicky, S. Kirkpatrick, and H. Ehrenreich, Phys. Rev. 175, 747 (1968).
[27]N. J. Shevchik and W. Paul, J. Non-Cryst. Solids 13, 1 (1973).
[28]F. W. Lytle, D. C. Sayers, and E. A. Stern, Phys. Rev. B 11, 4825 (1975).
[29]C. Ribbing, D. T. Pierce and W. E. Spicer, Phys. Rev. B 4, 4417 (1972).
[30]C. N. Bergland and W. E. Spicer, Phys. Rev. 136, A1030 (1964).
[31]R. S. Nelson and D. J. Mazey, in *Ion Surface Interaction, Sputtering and Related Phenomena*, edited by R. Behrisch *et al.*, (Gordon and Breach, New York, 1973).
[32]N. V. Smith, Phys. Rev. B 4, 1365 (1974).
[33]R. S. Williams, P. S. Wehner, J. Stöhr, and D. A. Shirley, Phys. Rev. Lett. 39, 302 (1977).